Int J Clin Exp Med 2016;9(11):21346-21357
www.ijcem.com /ISSN:1940-5901/IJCEM0034905

Original Article

Establishing a patient-derived colorectal cancer xenograft model for translational research

Zhonghai Guan[1], Xiangheng Chen[2], Xiaoxia Jiang[1], Zhongqi Li[1], Xiongfei Yu[1], Ketao Jin[3], Jiang Cao[4], Lisong Teng[1]

[1]Department of Surgical Oncology, The First Affiliated Hospital, College of Medicine, Zhejiang University, Hangzhou 310000, Zhejiang, People's Republic of China; [2]Department of Minimally Invasive Surgery, The Second Xiangya Hospital of Central South University, Changsha 421001, Hunan, People's Republic of China; [3]Department of Gastrointestinal Surgery, Shaoxing People's Hospital, Shaoxing Hospital of Zhejiang University, Shaoxing 312000, Zhejiang Province, People's Republic of China; [4]Clinical Research Center, The 2nd Affiliated Hospital, School of Medicine, Zhejiang University, People's Republic of China

Received July 3, 2016; Accepted September 28, 2016; Epub November 15, 2016; Published November 30, 2016

Abstract: Colorectal cancer (CRC) remains to present a high incidence and mortality rate, despite of the advances in current targeted theraputic approaches. Accumulating studies indicates that Patient-derived xenograft (PDX) is an important cancer research tool for more personalized precision medicine. In this study, eighty five CRC tumors derived from Chinese patients were transplanted into BALB/c nude mice for PDX models establishment. Immunohistochemical and molecular investigations (such as, Sanger sequencing, AmpliSeq Cancer Hotspot Panel Version 2 and Proteomics) were performed to verify if the PDX retained both features from the patient. Then, PDX (the first generation) initiation engraftment rate and speed related pathologic and genetic factors were explored. We found that 50 out of 85 (58.5%) CRC tumors successfully engrafted. A high genetic concordance between patient donor tumor and PDX was confirmed by pathologic, genetic, and proteomics investigations. CRC tumor staging, tumor location, somatic mutations were correlated with PDX initiation engraftment rate and speed. In conclusion, we established 50 CRC PDX models with a high histologic and genetic representativeness of the primary tumor. This platform will represent a reliable tool for CRC precision medicine and cancer translational research.

Keywords: Patient-derived xenograft model, colorectal cancer, precision medicine, translational research

Introduction

Colorectal cancer (CRC) is the fourth cause of cancer-related deaths worldwide. Early diagnosis and treatment have improved survival of colorectal cancer, but the 5-year survival of metastatic (i.e., Stage IV) CRC remains less than 10% (see http://globocan.iarc.fr/Pages/fact_sheets_cancer.aspx) [1]. It is estimated that about 376,300 Chinese will be diagnosed of colorectal cancer in 2015 and 191,000 of whom will succumb to this disease, corresponding to 51 colorectal cancer deaths on average per day [2]. Besides of the mainstay treatment surgery, chemotherapy and radiotherapy for patients with rectal cancer, substantial improvements have been made in the treatment of metastatic colorectal cancer during the past two decades, due to the introduction of targeted agents [3, 4]. However, in fact, not all patients benefit from current therapies, thus more personalized medicine appoaches remain to be developed [5, 6].

Preclinical evaluation of cancer targeted agents highly depend on drug evaluation animal models [7]. However, the cell-line derived xenograft models, which have been commonly used for decades, no longer preserve the original genetic characteristics and show tumor heterogeneity, as a result of prolonged in vitro artificial culturing [8]. About 85% preclinical agents fail to demonstrate sufficient safety or efficacy for regulatory approval to enter clinical trials, due to lack of animal models well replicating the diversity of human cancer biology [9, 10]. Therefore, a more clinical-representative and more stable drug evaluation animal model will be urgently needed.

In recent years, patient-derived xenografts (PDXs), so-called Avatar models, have been widely used in various cancers for translational research [11]. PDXs are established by directly transplanting fresh patient tumor tissue into immune-compromised mice [12]. Accumulating evidences indicate that PDX models can maintain major pathological and molecular characteristic of the original tumor [7], thus to be an important tool for cancer precision medicine and translational research, including drug screening, personalized medicine applications, biomarker development, understanding of mechanisms of drug resistance and prospectively identification of clinical translation hypotheses [13].

In this study, we successfully established 50 CRC PDXs. The initiation engraftment rate of the PDX models was 58.8%. These models maintained the patient pathological and molecular characteristics and effectively reflected the patient tumor heterogeneity. In addition, we explored initiation engraftment rate and speed related clinicopathologic and molecular factors. Our established CRC PDX models platform is a superior tool for colorectal cancer precision medicine and translational research.

Materials and methods

Patients and tumor tissues

Eighty five tumor tissue specimens (labelled as C01-85) were obtained at initial surgery after primarily diagnosed during 2014-2015, from the First Affiliated Hospital, College of Medicine, Zhejiang University. The patients had not received chemotherapy or radiation therapy before surgery. The study was approved by the Scientific and Ethical Committee of the First Affiliated Hospital, College of Medicine, Zhejiang University. Fresh Surgical tumor specimen were separated into 3 parts. The first part of the tumors were immediately transported in nutrient solution to the laboratory animal center of Zhejiang University for xenografts implantation within 1 hour. The second part of the tumors were immediately frozen in liquid nitrogen, and then frozen at -80°C for genetic and protein analyses. The third part of the tumors were embedded in paraffin for histopathologic examination and immunohistochemical analysis.

Establishment of xenografts

Three-to-four-week-old female BALB/c nude mice were purchased from Slaccas (Shanghai Slaccas Laboratory Animal) and housed in SPF laboratory animal rooms at laboratory animal center of Zhejiang University. Mice were acclimated to new environments for at least 3 days before use. Surgical tumor tissues were cut into pieces of 3 to 4 mm and transplanted within 30 min s.c. to 4 mice. Additional tissues were snap-frozen and stored at -80°C until use. Animals were monitored periodically for their weight with an electronic balance and tumor growth with a Vernier caliper twice every week. The tumor volume was calculated as formula V = LD × (SD) 2/2, where V represents the tumor volume, LD and SD are the longest and the shortest tumor diameter respectively. Tumors were then harvested, minced and re-implanted as described above for passaging. At each generation, tumors were harvested and stored in liquid nitrogen and used for further experiments. The use of experimental animals adhered to the Principles of Laboratory Animal Care (NIH publication #85-23, revised in 1985). All animal studies were approved by the Institutional Animal Care and Use Committee of Zhejiang University (approval ID: SYXK(ZHE)-2005-0072).

Histological and immunohistochemical analysis

All of the slides were stained with Harris hematoxylin after dewaxing the 5-μm sections with dimethylbenzene and were evaluated by two pathologists. Specimen were fixed in 10% neutral formalin, embedded in paraffin, sectioned (5 μm thick) and placed on slides for marker analysis. After blocking nonspecific antibody binding, sections were incubated with the primary antibodies against CEA (CST), CK7 (CST), ki67 (CST), VEGF (Epitomics Inc), FGFR2 (Abcam), VEGFR2 (Abcam) overnight at 4°C. Immunohistochemistry was performed according to the streptavidin-biotin peroxidase complex method (Lab Vision). The slides were photographed using an Olympus BX60 (Olympus).

DNA isolation and mutation analysis

DNA samples were isolated by DNeasy Blood & Tissue Kit (50) Qiagen 69504. Isolated DNA samples were amplified by PCR for 13 exons of

the 5 selected genes (APC exon15 religion B, P53 exon5-6, KRAS exon2, NRAS exon2, BRAF exon15, PIK3CA exon9, EGFR exon19) on an Applied Biosystems Veriti™ 96 well Thermal Cycler instrument (Applied Biosystems). The primers were designed to using the software Primer Premier 5.0. Primer sequences are shown in Supplementary Table 2. DNA extraction and Sanger sequencing were performed for all 85 original tumor samples. PCR was performed in a 25 μl mixture as per the following procedure: denaturation at 95 C for 5 min; 35 cycles of denaturation at 94°C for 30 s, annealing at 55°C for 40 s, and extension at 72°C for 1 min; and a final extension at 72°C for 5 min. All PCR products analysis, purification and Sanger sequencing was performed by TSINGKE Biological Technology (Beijing, China). The sequences were scrutinized for variations alongside reference sequences using SeqMan Pro module of DNAstar 7.0 software.

Ion-torrent personal genome machine sequencing

AmpliSeq Cancer Hotspot Panel Version 2 (Life Technologies) specifically targets 50 cancer-associated genes, most of which are tumor suppressor genes and oncogenes, and harbors 2855 COSMIC hotspots [14]. In brief, 10 ng of DNA was extracted for the amplicon libraries using the Ion AmpliSeq™ 2.0 technology. The libraries were bar-coded (Ion Xpress™ barcode adapters, Life Technologies), clonally amplified by emulsion PCR in vitro (Ion OneTouch™ 200 Template Kit Version 2.0, Life Technologies), and sequenced on an Ion 318 Chip. Sequencing reads were first aligned to Human Genome version 19 (hg19) using Torrent Suite 4.2. Identification of variants was facilitated by using the IT Variant Caller software plugin (Life Technologies), and advanced annotation was performed by ANNOVAR software (openbioinformatics.org). Variants were selected by mutation type if they belonged to nonsynonymous or frameshift or stopgain at the exonic region. Variants with amino acid changes were further examined for whether the changes were potentially damaging alterations by well-known tools (SIFT, Polyphen2, LRT, MutationTaster). Variants were ranked as deleterious (labelled in black colour in figures) when simultaneously met all of the following conditions, SIFT (<0.05), pp2_HDIV (D/P), pp2_HVAR (D/P), LRT (D), MutationTaster (A/D), and those simultaneously met more than 3 conditions were ranked as high risk SNV (labelled in red colour in figures). Synonymous SNV were labelled as green.

Proteomics

Subsequently 100 mg of tissues from xenografts and correponding patients tumors were finely chopped and homogenised in 500 μl of lysis solution (4% SDS + 100 mM Tris/HCl pH 7.6 + 0.1 M DTT) and incubation at 95°C for 3 min, centrifugation at 16,000 × g for 5 min. Total proteins from each sample were extracted by the modified method of Filter-aided sample preparation, FASP. The samples were desalted with C18 spin tips and freeze-dried. All prepared samples were stored at -80°C until LC–MS/MS analysis. The label-free liquid chromatography mass spectrometric (LC-MS/MS) analysis of samples was performed using a Easy nanoLC 1000 coupled to a LTQ-Orbitrap Elite mass spectrometer (Thermo Fisher Scientific). Peptide mixtures (2 μg) were loaded by an auto-sampler. The peptide samples were subsequently eluted with a five-step linear gradient of A/B mixture (A: ddH_2O with 0.1% formic acid, B: ACN with 0.1% formic acid): 0-10 min, 3-8% B; 10-120 min, 8-20% B; 120-137 min, 20-30% B; 137-143 min, 30-90% B; 143-150 min, 90% B. The column flow was maintained as 250 nl/min. The chromatographic system was composed of a trapping column (75 μm × 2 cm, nanoviper, C18, 3 μM, 100 A) and an analytical column (50 μm × 15 cm, nanoviper, C18, 2 μM, 100 A). Data were acquired with Xcalibur software (Thermo Fisher Scientific). The mass spectrometer was operated in the positive mode and Nanospray Flex ionization source and FTMS analyzer combined with Thermo LTQ-Orbitrap Elite equipped Ion Trap analyzer. The parameters for FTMS were as follows: Data collection were at 30 K for the full scan MS, positive as polarity, profile as data type, and then proceeded to isolate the top 20 ions for MS/MS by CID (1.0 m/z isolation width, 35% collision energy, 0.25 activation Q, 10 ms activation time). Scan Range was set as 300 m/z First Mass and 2000 m/z Last Mass. All searches were performed using PEAKS v7.5 (Bioinformatics Solutions Inc) against a last vesion human uniprot protein database and common contaminant proteins (cRAP.fasta, 1/2015). Peptides were filtered with 0.5% FDR using a decoy database approach, and at least 1

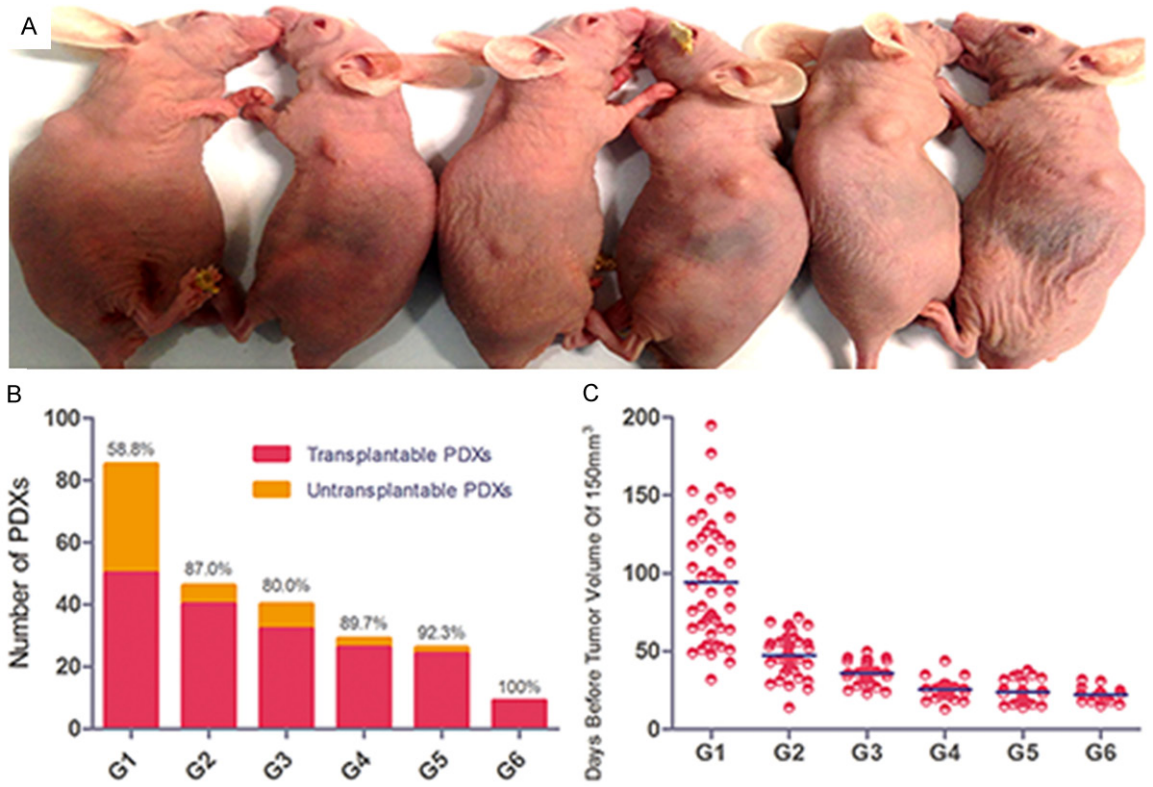

Figure 1. Establishment of xenografts & statistical observation of xenografts growth in mice. A. Xenografts established with BALB/c nude mice. B. PDX engraftment rate of each generation. C. Days cost for each generation engrafted PDX model to generate a 150 mm^3 tumor.

unique peptide and 2 total peptides per protein were required for protein assignments. The signification protein were filtered with ≥20 (-10lgP). cRAP contaminant database identified dust/contact proteins were removed from the table for clarity. Functional annotation and classification of all identified proteins were determined by using the Blast2 GO program against a last vesion human uniprot protein database.

Statistical analysis

Calculation and statistics were performed with Excel 2010 (Microsoft, Redmond, WA) and GraphPad Prism 5 (GraphPad Software, San Diego, CA). Experimental values were reported as mean ± SD. Column analyses correlation in GraphPad Prism 5 was used for statistical analysis of the engraftment success rate and speed related factors. $P<0.05$ was considered statistically significant.

Results

Patient characteristics

From June 2014 to December 2014, CRC (colorectal cancer) tumor tissues obtained from a total of 85 operation patients (labelled as C01-85) were subcutaneously implanted into BALB/c nude mice for PDX models establishment (**Figure 1A**). Clinical and pathologic characteristics are described in **Table 1**. Totally 50 tumors out of 85 (58.8%) were successfully engrafted.

Growth of CRC xenografts in BALB/c mice

Primary tumors was engrafted in mice at the first generation after average 3 months; tumor was re-implanted in new mice after reaching a volume of 1000 mm^3. PDXs were serially passaged in animals 3-5 times. The engraftment rate rose above 80% from the second generation (**Figure 1B**). We set the time from tumor tissue transplantation until tumor volume 150 mm^3 as the endpoint of engraftment speed evaluation. The 50 first generation engrafted PDX models costed average 94.3 days to generate a 150 mm^3 tumor. Then, starting from the second generation, the latency of engraftment decreased from 3 months to 1.5 month until the stabilization obtained at the fourth generation (**Figure 1C**).

Table 1. Clinical-pathological characteristics of CRC patients (N=85)

Characteristics	Patients, n (%)
Gender	
Male	53 (62.4)
Female	32 (37.6)
Age, y	
Median (range)	63.1 (36-84)
Primary site	
Right hemicolon	12 (14.1)
Colon transversum	4 (4.7)
Left hemicolon	2 (2.4)
Sigmoideum	25 (29.4)
Rectum	42 (49.4)
Dukes staging	
A1	1 (1.2)
A2	1 (1.2)
A3	12 (14.1)
B	35 (41.2)
C1	31 (36.5)
C2	2 (2.3)
D	3 (3.5)
Macroscopic type	
Infiltrative	1 (1.2)
Protuberant	18 (21.2)
Ulcerated	66 (77.6)
Pathologic type	
Adenocarcinoma	76 (89.4)
Mucinous adenocarcinoma	9 (10.6)
Tumor differentiation	
Moderate	63 (74.1)
Moderate-poor	20 (23.5)
Poor	2 (2.4)
Gene mutation status	
KRAS	17 (20)
NRAS	1 (1.2)
BRAF	4 (4.7)
PIK3CA	6 (7.1)
EGFR	19 (22.4)
APC	38 (44.7)
P53	36 (42.4)
Engrafted mode	
Yes	50 (58.8)
No	35 (41.2)
Days before tumor volume 150 mm^3	
Median (range)	94.3 (32-195)

Comparison of the histology and immmunohistochemistry between the xenografts and the patient tumors

In order to further evaluate the PDX xenografts, immunohistochemical and molecular test were performed to identify if both characteristics were retained in the PDX. Immunohistochemical expressions of CEA, CK7, ki67, VEGF, FGFR2 and VEGFR2 as well as the HE staining showed that the pathological characteristics of the third passage xenografts were in accordance with the original patient samples (**Figure 2A**). Cancer related somatic mutations were identified in one primary patient tumor sample and corresponding PDX tumor tissue. The PDX tumor manifested the same somatic gene mutations with original patient, such as KRAS (A59T), TP53 (R175C), SMARCB1 (R374W) (**Figure 2B**, detailed data shown in Supplementary Table 1). The comparison between original patient tumor and its PDX revealed a high accordance in terms of proteomic analysis (**Figure 2C**). To gain insights into the biological changes in the PDX tumor compared with the original patient tumor, the differentially expressed proteins were categorized as per the Gene Ontology (GO) classes, such as cellular component, molecular function and biological process. GO analysis of the differentially expressed proteins concentrated upon 18 GO terms, as follows, defense response, response to wounding, regulation of locomotion, regulation of response to external stimulus, regulation of cytokine production, inflammatory response, response to bacterium, regulation of inflammatory response, leukocyte migration, negative regulation of response to stimulus, defense response to bacterium, negative regulation of defense response, regulation of cytokine biosynthetic process, positive regulation of cytokine biosynthetic process, regulation of behavior, regulation of chemotaxis, regulation of chemokine production, and regulation of chemokine biosynthetic process (**Figure 2D**).

The initiation PDX engraftment rate related factors

Column analyses correlation was used for statistical analysis of the engraftment success rate related factors. We found that higher Dukes staging and TNM staging were positive correlated with successful engraftment ($P< 0.05$, **Figure 3A**, **3B**). Colon cancer demonstrated a higher PDX engraftment success rate (65.1%, 28/43) than rectum cancer (52.4%, 22/42) (**Figure 3E**). Then, 85 original patient tumor were detected for mutations of *APC* exon15 religion B, *TP53* exon5-6, *KRAS* exon2, *NRAS* exon2, *BRAF* exon15, *PIK3CA* exon9 and *EGFR* exon19. We compared the mutations fre-

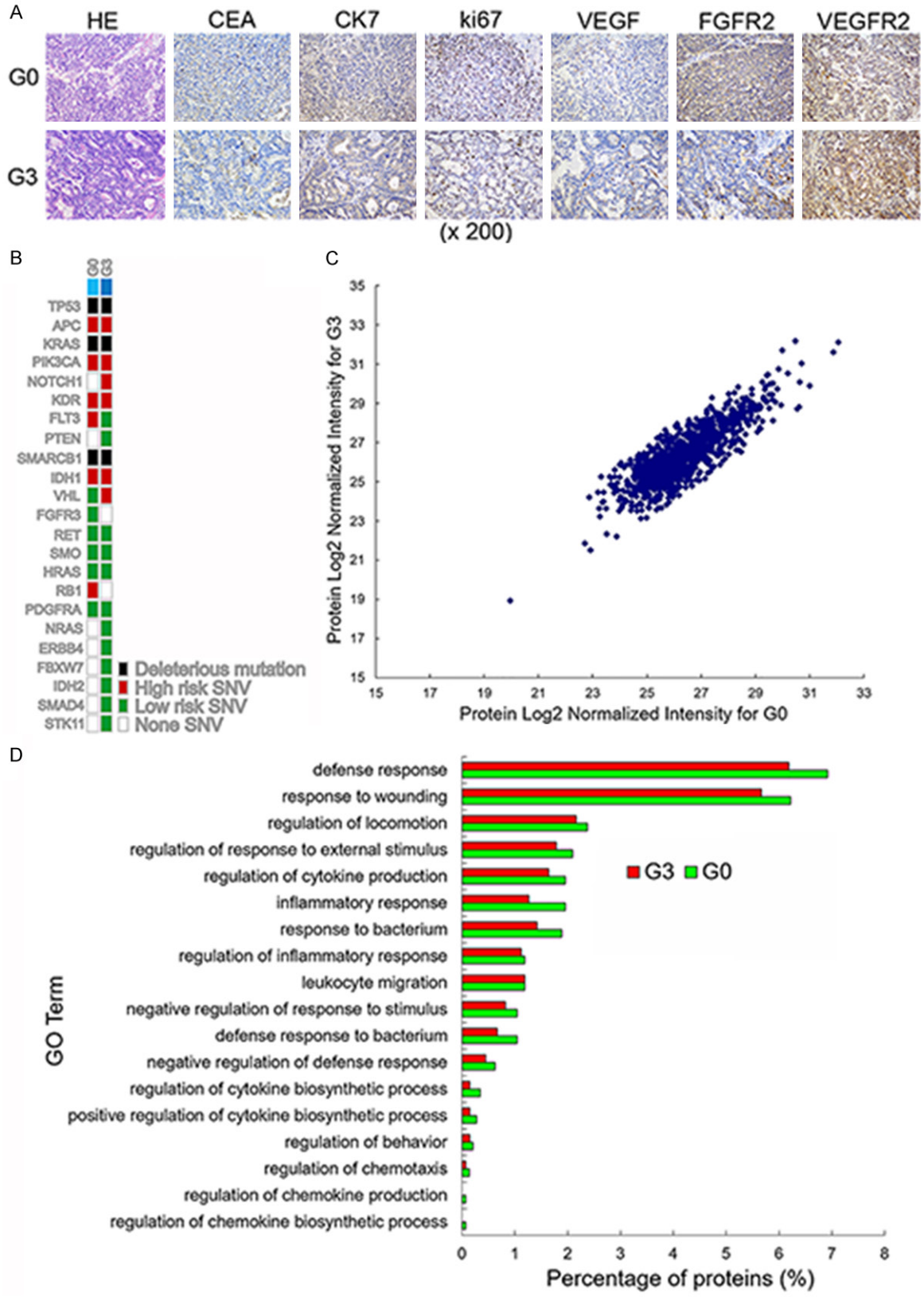

Figure 2. Comparison of the histology and immmunohistochemistry between the xenografts and the patient tumors. A. Immunohistochemical expressions of CEA, CK7, ki67, VEGF, FGFR2 and VEGFR2 as well as the HE staining showed that the pathological characteristics of the third passage xenografts were in accordance with the original patient samples. B. The PDX tumor manifested the same somatic gene mutations with original patient. C. The com-

parison between original patient tumor and its PDX revealed a high accordance in terms of proteomic analysis. D. GO analysis of the differentially expressed proteins concentrated upon 18 GO terms.

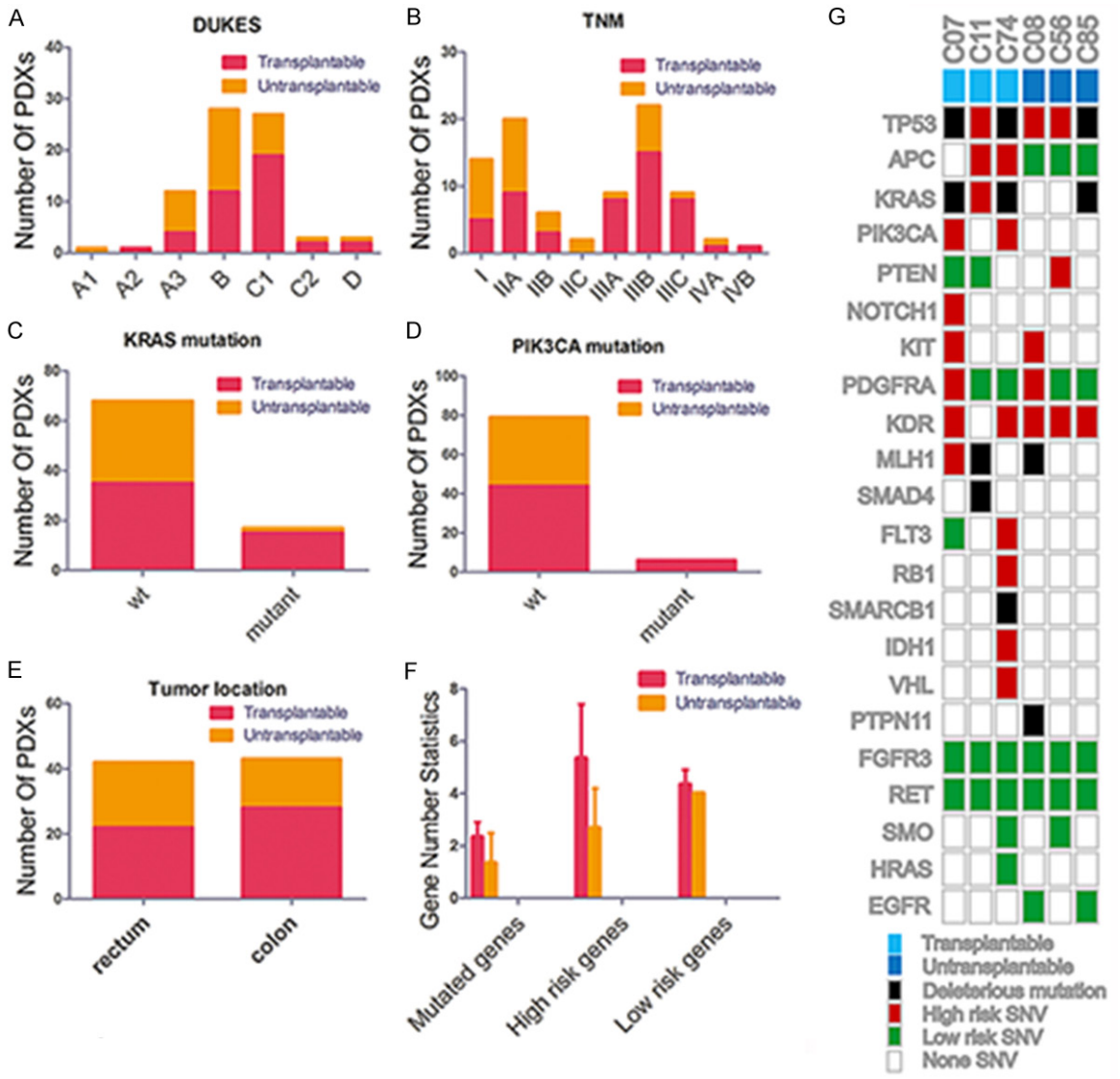

Figure 3. The initiation PDX engraftment success rate related factors. A, B. Higher Dukes staging and TNM staging were positive correlated with successful engraftment (P<0.05). C, D. *KRAS* (P<0.01) and *PIK3CA* (P<0.05) mutation were positive correlated with successful engraftment. E. Colon cancer demonstrated a higher PDX engraftment success rate (65.1%, 28/43) than rectum cancerv (52.4%, 22/42). F, G. Statistical analysis of deleterious mutated genes, high risk and low risk genes between 3 original patient tumors with the highest engraftment success rate and another 3 with the lowest engraftment success rate in terms of tumor associated hot spot mutation.

quency between 50 successful engraftment patient tumor (namely, transplantable tumor) and 35 untransplantable tumors. Among the detected genes, *KRAS* (P<0.01) and *PIK3CA* (P<0.05) mutation were positive correlated with successful engraftment (**Figure 3C**, **3D**). To further explore the engraftment rate related molecular factors of the first generation PDX engraftment, 3 original patient tumors with the highest engraftment success rate (all 4 transplanted mice successfully engrafted) were compared with another 3 with the lowest engraftment success rate (none of 4 transplanted mice engrafted) in terms of tumor associated hot spot mutation, to find that the former appeared to have more deleterious

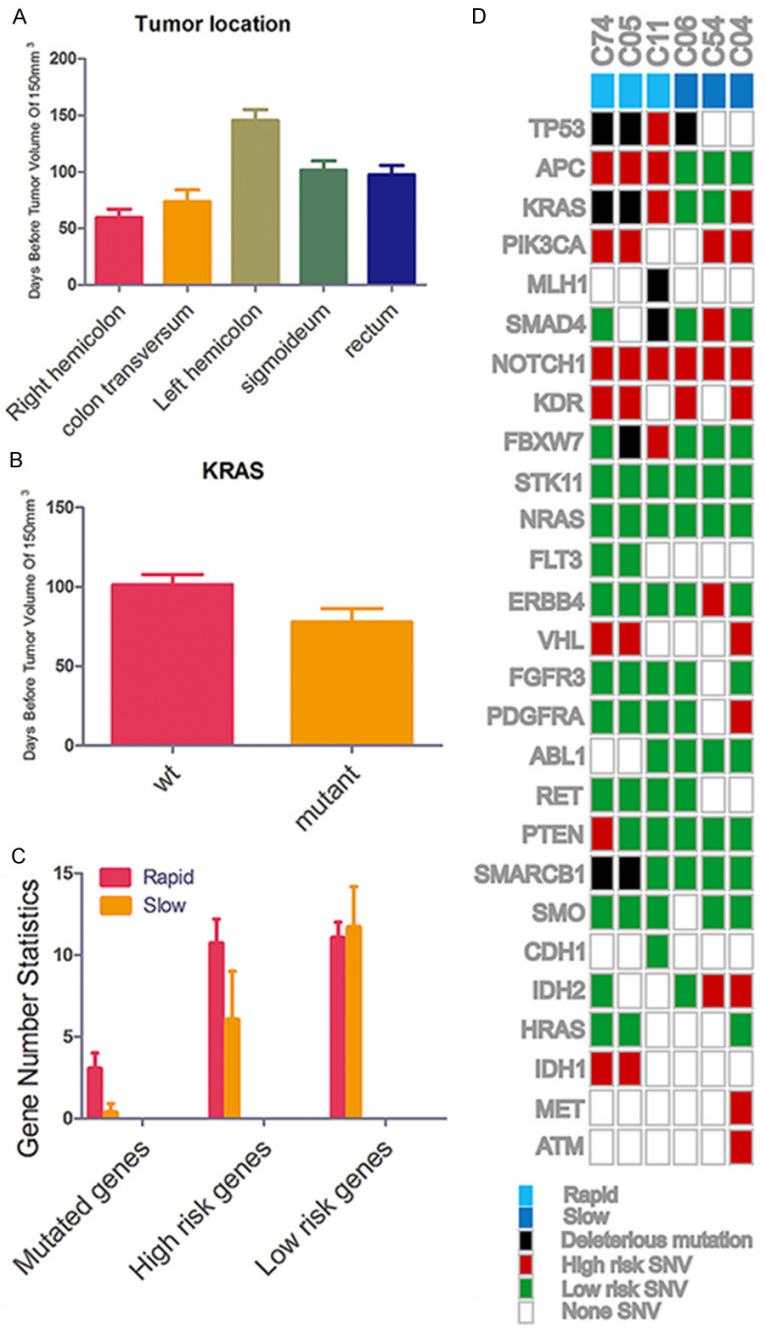

Figure 4. The initiation PDX engraftment speed related factors. A. Tumors from left hemi-colon appeared to have a faster engraftment speed than tumors from other locations. B. *KRAS* ($P<0.05$) mutation were positive correlated with engraftment speed. C, D. The 3 original patient tumors (C74, C05, C11) with the fastest engraftment speed appeared to have more deleterious mutated genes (shown in black colour) and high risk SNV genes (shown in red colour) than another 3 (C06, C54, C04) with the slowest engraftment speed.

mutated genes (shown in black colour) and high risk SNV genes (shown in red colour) (**Figure 3F**, **3G**).

The initiation PDX engraftment speed related factors

The latencies of engraftment and growth rates of PDXs varied significantly among different models (**Table 1**). Among the 50 transplantable PDX models, we compared 15 rapid-growth models which showed earliest tumor growth after transplantion (average 54.1 days) with 15 slow-growth models (average 142.3 days). Similar with engraftment rate related factors, we found that tumor location were correlated with PDX engraftment speed. Tumors from left hemi-colon appeared to have a faster engraftment speed than tumors from other locations (**Figure 4A**), while tumor staging factor had no statistical significance. *KRAS* ($P<0.05$) mutation were positive correlated with engraftment speed (**Figure 4B**). To further explore engraftment speed related molecular factors of the first generation PDX engraftment, 3 original patient tumors (C74, C05, C11) with the fastest engraftment speed were compared with another 3 (C06, C54, C04) with the slowest engraftment speed (Supplemental Figure 1) in terms of tumor associated hot spot mutation, to find that the former appeared to have more deleterious mutated genes (shown in black colour) and high risk SNV genes (shown in red colour) (**Figure 4C**, **4D**).

Discussion

There has been a notable expansion of precision-medicine programmes in recent years [15, 16]. Novel cancer targeted agents research requires a more clinical-representative drug evaluation

animal models which well replicates the diversity of patient cancer biology [9]. PDX models represent enhanced preclinical tools with more imitation of human cancer biology and patient response to treatments [17].

Typically, PDX initiation engraftment rates vary between 25 and 60% with different tumor types [18]. In our study, we successfully established 50 CRC PDXs, with engraftment rate of 58.8%, using BALB/c nude mice as hosts and CRC tumor tissues only obtained from primary colorectal cancer. It was reported the engraftment rate of colorectal cancer PDXs reached 70% or so [19-21]. We attributed these different results mainly to the usage of different types of hosts and tumor origin [22]. PDXs were serially passaged in animals 3-5 times. In our study, the engraftment rate rose above 80% from the second generation (**Figure 1B**). As the human stromal tissue in the PDX models gradually replaced by murine stromal tissue during tumor passaging, associated immune response will be blunted, facilitating the engraftment rate [23]. In our study, 50 first generation engrafted PDX models costed average 94.3 days to generate a 150 mm^3 tumor. Then, starting from the second generation, the latency of growth decreased from 3 months to 1.5 month until obtaining a stabilization at the fourth generation. The gradually rise of engraftment rate and speed indicate that, once engrafted, PDXs can be easily transplanted from mouse to mouse, which will make it feasible to conduct several experimental replicates [24].

Animal models which better recapitulate the heterogeneity of tumours in patients will therefore be more predictive [7]. An important question regarding PDX model stability is whether the engraftment or expansion changes the molecular features of the tumours. In our study, The PDX tumor not only showed the basically same immunohistochemical expression of CEA, CK7, ki67, VEGF, FGFR2 and VEGFR2 by as well as the Hematoxillin & Eosin staining, but also somatic mutations with the original patient. In order to further validate and explore the PDX model stability, we compared the PDX with corresponding donor patient tumor by proteomic analysis, revealing a high correlation of majority proteins. Therefore, we demonstrated that the PDX retained most of primary tumor genetic characteristics in terms of pathological, genetic and protomic characteristics. All these results above indicate that we successfully established a CRC PDX models platform, which retained the patient molecular characteristics and reflected the patient tumor heterogeneity.

Another question is whether the different characteristics are generated by tumor evolution and whether these differences influence the stability of the model clinico-representativeness. In our study, IT-PGM sequencing of one model showed that PDX tumor retained the same deleterious somatic mutations from the donor patient, while heterogenicity were present for genes with high risk SNV (shown in red colour) or synonymous SNV (shown in green colour) (**Figure 2B**). These high risk nonsynonymous SNV and synonymous SNV are usually considered to have no contribution to disease, and mechanisms might be more likely due to selection of pre-existing clones, rather than the evolutional generation of new clones [25-27]. Further, we utilized proteomics assay to take a sight into the different expressed proteins between the PDX tumors and patient tumors. In our study, GO analysis of the differentially expressed proteins in the PDX tumor compared with the original patient tumor concentrated upon 18 GO terms, the majority of which were related to immunologic and inflammatory function. In each of the 18 GO terms, proteins in PDX tumor were wholly fewer than those in the primary tumor, which reflected the lack of an immune system and were likely to have a substantial role in forming the selection pressures for engrafted tumour tissues (**Figure 2D**) [13]. The results above indicate that the differences between PDX and origin tumor mainly reflect the interreaction between transplants and hosts, demonstrating the stable clinical-representativeness of PDX models.

The ultimate goal of Avatar models utilization should be guiding clinical decisions. However, about 30% of patients cannot generate an Avatar model. Another attention-getting question considering that some patients would not benefit from the experimental findings before disease progression and death, particularly for more aggressive cancer patients [13]. In fact, PDX engraftment rate and speed can be quite variable and unpredictable, especially in less aggressive tumors [7, 12]. In order to better optimize the strategy of PDX-based personalized precision medicine research, more individ-

ualized PDX model establishment methodology should be considered in practice, that is to say, different animal host type, implantation location, tumor tissue management should be utilized for different type of patient tumor. Therefore, in this study, we compared engraftment rate and speed among different patients in terms of demographic characteristics. We showed that tumor location, *KRAS* mutation, *PIK3CA* mutation, as well as cancer hotspot mutated genes number are correlated with PDX engraftment rate (**Figure 3**). Few studies have evaluated the relationship between the PDX engraftment speed, namely tumor-take time. In our study, we showed that tumors location, *KRAS* ($P<0.05$) mutation and cancer hotspot mutated genes number are correlated with engraftment speed (**Figure 4**). The *KRAS* mutation has been reported to be positive correlated with engraftment rate in colorectal cancer PDX models [28, 29], while we showed *PIK3CA* mutation positive correlated with PDX engraftment rate and *KRAS* mutation is also positive correlated with PDX engraftment speed. In our study, we first showed that more deleterious mutated genes number indicates higher PDX engraftment rate and speed by AmpliSeq Cancer Hotspot Panel Version 2. Logically speaking, the more progressive and metastatic colorectal cancer tends to be, the more need for precision medicine there will be. In our study, we found that CRC tumor staging, tumor location, somatic mutaions were correlated with engraftment success rate and speed. More malignant and invasive CRC tended to have a higher engraftment success rate and speed, which seem to be a positive indication [30, 31]. For less advanced cancers, the clinical utility of CRC xenograft engraftment may be limited by low engraftment rates and speed [7]. Therefore, in order to enhance PDX engraftment rates and speed for the less advanced cancers, more researches will be needed for a comprehensive comparison among different hosts, different implantation locations and tumor tissue management, with regards to engraftment rate, engraftment speed, thus to provide an optimum selection for different type of tumors [22]. Further, the standard operating procedures for different type of tumors are needed [24].

In conclusion, we successfully established 50 CRC PDXs. The success rate of the PDX models was 58.8%. These PDX models retained the patient pathological and molecular characteristics and reflected the patient tumor heterogeneity. We suggest that more individualized PDX model establishment methodology should be established for colorectal cancer precision medicine.

Acknowledgements

This work was partially supported by National Science and Technology Major Project of the Ministry of Science and Technology of China (Grant No. 2013ZX09506015), National Natural Science Foundation of China (Grant No. 81272676), National Natural Science Foundation of China (Grant No. 81374014), Zhejiang Provincial Natural Science Foundation (Grant No. LY15H160012), Zhejiang Provincial Natural Science Foundation (Grant No. LY15H160026) and Zhejiang Provincial Medical and Healthy Science and Technology Projects (Grant No. 2013KYA228).

Disclosure of conflict of interest

None.

Address correspondence to: Lisong Teng, Department of Surgical Oncology, First Affiliated Hospital, College of Medicine, Zhejiang University, 79 Qingchun Road, Hangzhou 310003, Zhejiang, People's Republic of China. Tel: +86 571 8706 8873; +86 136 6667 6918; Fax: +86 571 8723 6628; E-mail: lsteng@zju.edu.cn

References

[1] Torre LA BF, Siegel RL, Ferlay J, Lortet-Tieulent J, Jemal A. Global cancer statistics, 2012. CA Cancer J Clin 2015; 65: 87-108.

[2] Chen W, Zheng R, Baade PD, Zhang S, Zeng H, Bray F, Jemal A, Yu XQ, He J. Cancer statistics in China, 2015. CA Cancer J Clin 2016; 66: 115-32.

[3] Schmoll HJ, Van Cutsem E, Stein A, Valentini V, Glimelius B, Haustermans K, Nordlinger B, van de Velde CJ, Balmana J, Regula J, Nagtegaal ID, Beets-Tan RG, Arnold D, Ciardiello F, Hoff P, Kerr D, Köhne CH, Labianca R, Price T, Scheithauer W, Sobrero A, Tabernero J, Aderka D, Barroso S, Bodoky G, Douillard JY, El Ghazaly H, Gallardo J, Garin A, Glynne-Jones R, Jordan K, Meshcheryakov A, Papamichail D, Pfeiffer P, Souglakos I, Turhal S, Cervantes A. ESMO Consensus Guidelines for management of patients with colon and rectal cancer. a per-

sonalized approach to clinical decision making. Ann Oncol 2012; 23: 2479-516.
[4] Brenner H, Kloor M, Pox CP. Colorectal cancer. Lancet 2014; 383: 1490-502.
[5] Chong CR, Jänne PA. The quest to overcome resistance to EGFR-targeted therapies in cancer. Nat Med 2013; 19: 1389-400.
[6] Oddo D, Sennott EM, Barault L, Valtorta E, Arena S, Cassingena A, Filiciotto G, Marzolla G, Elez E, van Geel RM, Bartolini A, Crisafulli G, Boscaro V, Godfrey JT, Buscarino M, Cancelliere C, Linnebacher M, Corti G, Truini M, Siravegna G, Grasselli J, Gallicchio M, Bernards R, Schellens JH, Tabernero J, Engelman JA, Sartore-Bianchi A, Bardelli A, Siena S, Corcoran RB, Di Nicolantonio F. Molecular landscape of acquired resistance to targeted therapy combinations in BRAF-mutant colorectal cancer. Cancer Res 2016; 76: 4504-15.
[7] Johnson JI, Decker S, Zaharevitz D, Rubinstein LV, Venditti JM, Schepartz S, Kalyandrug S, Christian M, Arbuck S, Hollingshead M, Sausville EA. Relationships between drug activity in NCI preclinical in vitro and in vivo models and early clinical trials. Br J Cancer 2001; 84: 1424-31.
[8] Wilding JL, Bodmer WF. Cancer cell lines for drug discovery and development. Cancer Res 2014; 74: 2377-84.
[9] Arrowsmith J, Miller P. Trial Watch: Phase II and Phase III attrition rates 2011-2012. Nat Rev Drug Discov 2013; 12: 569.
[10] Arrowsmith J. Trial watch: Phase II failures: 2008-2010. Nat Rev Drug Discov 2011; 10: 328-9.
[11] Hidalgo M, Bruckheimer E, Rajeshkumar NV, Garrido-Laguna I, De Oliveira E, Rubio-Viqueira B, Strawn S, Wick MJ, Martell J, Sidransky D. A pilot clinical study of treatment guided by personalized tumorgrafts in patients with advanced cancer. Mol Cancer Ther 2011; 10: 1311-6.
[12] Morton CL, Houghton PJ. Establishment of human tumor xenografts in immunodeficient mice. Nat Protoc 2007; 2: 247-50.
[13] Aparicio S, Hidalgo M, Kung AL. Examining the utility of patientderived xenograft mouse models. Nat Rev Cancer 2015; 15: 311-6.
[14] Tsongalis GJ, Peterson JD, de Abreu FB, Tunkey CD, Gallagher TL, Strausbaugh LD, Wells WA, Amos CI. Routine use of the ion torrent AmpliSeq™ cancer hotspot panel for identification of clinically actionable somatic mutations. Clin Chem Lab Med 2014; 52: 707-714.
[15] Aronson SJ, Rehm HL. Building the foundation for genomics in precision medicine. Nature 2015; 526: 336-42.
[16] Garay JP, Gray JW. Omics and therapy-A basis for precision medicine. Mol Oncol 2012; 6: 128-39.
[17] Rosfjord E, Lucas J, Li G, Gerber HP. Advances in patient-derived tumor xenografts: from target identification to predicting clinical response rates in oncology. Biochem Pharmacol 2014; 91: 135-43.
[18] Siolas D, Hannon GJ. Patient-derived tumor xenografts: transforming clinical samples into mouse models. Cancer Res 2013; 73: 5315-9.
[19] Cho YB HH, Choi YL, Oh E, Joo KM, Jin J, Nam DH, Ko YH, Lee WY. Colorectal cancer patient-derived xenografted tumors maintain characteristic features of the original tumors. J Surg Res 2014; 187: 502-9.
[20] Dangles-Marie V, Pocard M, Richon S, Weiswald LB, Assayag F, Saulnier P, Judde JG, Janneau JL, Auger N, Validire P, Dutrillaux B, Praz F, Bellet D, Poupon MF. Establishment of human colon cancer cell lines from fresh tumors versus xenografts: comparison of success rate and cell line features. Cancer Res 2007; 67: 398-407.
[21] Linnebacher M, Maletzki C, Ostwald C, Klier U, Krohn M, Klar E, Prall F. Cryopreservation of human colorectal carcinomas prior to xenografting. BMC Cancer 2010; 10: 362.
[22] Tentler JJ, Tan AC, Weekes CD, Jimeno A, Leong S, Pitts TM, Arcaroli JJ, Messersmith WA, Eckhardt SG. Patient-derived tumour xenografts as models for oncology drug development. Nat Rev Clin Oncol 2012; 9: 338-50.
[23] Pearson AT, Finkel KA, Warner KA, Nör F, Tice D, Martins MD, Jackson TL, Nör JE. Patient-derived xenograft (PDX) tumors increase growth rate with time. Oncotarget 2016; 7: 7993-8005.
[24] Hidalgo M, Amant F, Biankin AV, Budinská E, Byrne AT, Caldas C, Clarke RB, de Jong S, Jonkers J, Mælandsmo GM, Roman-Roman S, Seoane J, Trusolino L, Villanueva A. Patient-Derived Xenograft Models: An Emerging Platform for Translational Cancer Research. Cancer Discov 2014; 4: 998-1013.
[25] Eirew P, Steif A, Khattra J, Ha G, Yap D, Farahani H, Gelmon K, Chia S, Mar C, Wan A, Laks E, Biele J, Shumansky K, Rosner J, McPherson A, Nielsen C, Roth AJ, Lefebvre C, Bashashati A, de Souza C, Siu C, Aniba R, Brimhall J, Oloumi A, Osako T, Bruna A, Sandoval JL, Algara T, Greenwood W, Leung K, Cheng H, Xue H, Wang Y, Lin D, Mungall AJ, Moore R, Zhao Y, Lorette J, Nguyen L, Huntsman D, Eaves CJ, Hansen C, Marra MA, Caldas C, Shah SP, Aparicio S. Dynamics of genomic clones in breast cancer patient xenografts at single-cell resolution. Nature 2015; 518: 422-6.

[26] Shah SP, Roth A, Goya R, Oloumi A, Ha G, Zhao Y, Turashvili G, Ding J, Tse K, Haffari G, Bashashati A, Prentice LM, Khattra J, Burleigh A, Yap D, Bernard V, McPherson A, Shumansky K, Crisan A, Giuliany R, Heravi-Moussavi A, Rosner J, Lai D, Birol I, Varhol R, Tam A, Dhalla N, Zeng T, Ma K, Chan SK, Griffith M, Moradian A, Cheng SW, Morin GB, Watson P, Gelmon K, Chia S, Chin SF, Curtis C, Rueda OM, Pharoah PD, Damaraju S, Mackey J, Hoon K, Harkins T, Tadigotla V, Sigaroudinia M, Gascard P, Tlsty T, Costello JF, Meyer IM, Eaves CJ, Wasserman WW, Jones S, Huntsman D, Hirst M, Caldas C, Marra MA, Aparicio S. The clonal and mutational evolution spectrum of primary triple-negative breast cancers. Nature 2012; 486: 395-9.

[27] Roth A, Khattra J, Yap D, Wan A, Laks E, Biele J, Ha G, Aparicio S, Bouchard-Côté A, Shah SP. PyClone: statistical inference of clonal population structure in cancer. Nat Methods 2014; 11: 396-8.

[28] Bertotti A, Migliardi G, Galimi F, Sassi F, Torti D, Isella C, Corà D, Di Nicolantonio F, Buscarino M, Petti C, Ribero D, Russolillo N, Muratore A, Massucco P, Pisacane A, Molinaro L, Valtorta E, Sartore-Bianchi A, Risio M, Capussotti L, Gambacorta M, Siena S, Medico E, Sapino A, Marsoni S, Comoglio PM, Bardelli A, Trusolino L. A molecularly annotated platform of patient-derived xenografts ("xenopatients") identifies HER2 as an effective therapeutic target in cetuximab-resistant colorectal cancer. Cancer Discov 2011; 1: 508-23.

[29] Cavalloni G, Peraldo-Neia C, Sassi F, Chiorino G, Sarotto I, Aglietta M, Leone F. Establishment of a patient-derived intrahepatic cholangiocarcinoma xenograft model with KRAS mutation. BMC Cancer 2016; 16: 90.

[30] Némati F, Sastre-Garau X, Laurent C, Couturier J, Mariani P, Desjardins L, Piperno-Neumann S, Lantz O, Asselain B, Plancher C, Robert D, Péguillet I, Donnadieu MH, Dahmani A, Bessard MA, Gentien D, Reyes C, Saule S, Barillot E, Roman-Roman S, Decaudin D. Establishment and Characterization of a Panel of Human Uveal Melanoma Xenografts Derived from Primary and/or Metastatic Tumors. Clin Cancer Res 2010; 16: 2352-62.

[31] Sivanand S, Peña-Llopis S, Zhao H, Kucejova B, Spence P, Pavia-Jimenez A, Yamasaki T, McBride DJ, Gillen J, Wolff NC, Morlock L, Lotan Y, Raj GV, Sagalowsky A, Margulis V, Cadeddu JA, Ross MT, Bentley DR, Kabbani W, Xie XJ, Kapur P, Williams NS, Brugarolas J. A validated tumorgraft model reveals activity of dovitinib against renal cell carcinoma. Sci Transl Med 2012; 4: 137ra75.

Supplementary Table 1. The deleterious mutations of PDX model by AmpliSeq Cancer Hotspot Panel Version 2

Gene	Exon	cDNA change	AAChange	COSMIC	Already reported	Mutation type	SIFT	pp2_HDIV	pp2_HVAR	LRT	MutationTaster
KRAS	3	c.G175A	p.A59T	COSM546	no	missense	0.01	P	P	D	D
TP53	5	c.C523T	p.R175C	COSM43680	no	missense	0	D	D	D	D
SMARCB1	9	c.C1120T	p.R374W	COSM1226778	no	missense	0	D	D	D	D

Abbreviations: D: damaging; P: probably damaging; B: benign. All mutations are Heterozygous.

Supplementary Table 2. The primers sequences designed by the software Primer Premier 5.0

KRAS exon2	Forward	TGTGTGACATGTTCTAATATAGTCACAT
	Reverse	GGTCCTGCACCAGTAATATGC
NRAS exon2	Forward	GTGAAATGACTGAGTACAAA
	Reverse	TATGGTGGGATCATATTC
IK3CA exon9	Forward	AGTAACAGACTAGCTAGAGA
	Reverse	ATTTTAGCACTTACCTGTGAC
BRAF exon15	Forward	TCATAATGCTTGCTCTGATAGGA
	Reverse	GGCCAAAAATTTAATCAGTGGA
EGFR exon19	Forward	CACAATTGCCAGTTAACGTCT
	Reverse	CCCACACAGCAAAGCAGA
APC exon15 religion B	Forward	AGGGTTCTAGTTTATCTTCA
	Reverse	TCTGCTTGGTGGCATGGTTT
P53 exon5-6	Forward	GGGTTGCAGGAGGTGCTT
	Reverse	TAAGCAGCAGGAGAAAGC

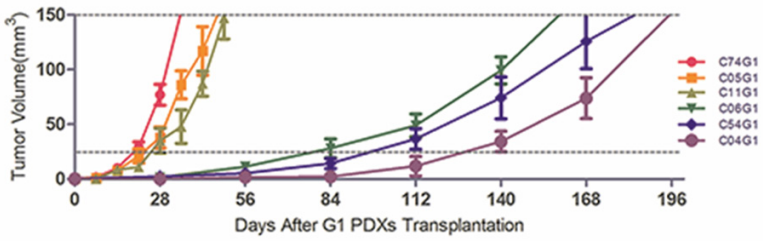

Supplementary Figure 1. Growth curve of 3 models with the fastest engraftment speed and another 3 models with the slowest engraftment speed.